Characterization of tetragonal distortion in a thick $Al_{0.2}Ga_{0.8}N$ epilayer with an AlN interlayer by Rutherford backscattering/channeling*

Wang Huan(王 欢)[a)b)] and Yao Shu-De(姚淑德)[a)†]

[a)] *State Key Laboratory of Nuclear Physics and Technology, Peking University, Beijing* 100871, *China*
[b)] *Chinese Academy of Engineering Physics, Mianyang* 621900, *China*

(Received 17 November 2013; revised manuscript received 23 February 2014; published online 23 July 2014)

An $Al_{0.2}Ga_{0.8}N/AlN/Al_{0.2}Ga_{0.8}N$ heterostructure was grown by metalorganic chemical vapor deposition on a sapphire (0001) substrate with a thick (> 1 μm) GaN intermediate layer. The Al composition was determined by Rutherford backscattering (RBS). Using the channeling scan around an off-normal $[1\bar{2}13]$ axis in the $(10\bar{1}0)$ plane of the $Al_{0.2}Ga_{0.8}N$ layer, the tetragonal distortion e_T, which is caused by the elastic strain in the epilayer, is investigated. The results show that e_T in the high-quality $Al_{0.2}Ga_{0.8}N$ layer is dramatically released by the AlN interlayer from 0.66% to 0.27%.

Keywords: AlGaN, Rutherford backscattering/channeling, elastic strain

PACS: 68.55.–a, 73.61.Ey, 82.80.Yc **DOI:** 10.1088/1674-1056/23/9/096801

1. Introduction

The growth of high-quality GaN on sapphire using a low-temperature buffer layer,[1] the realization of p-type nitride films using Mg as the dopant,[2] and the following special treatments[3] have led to the commercialization of nitride-based near-UV, blue and green light-emitting diodes and the achievement of violet laser diodes. Optoelectronics in the visible short-wavelength region have been established by nitrides. In the above devices, the active layer is usually InGaN-based quantum wells and the cladding layers are usually $Al_xGa_{1-x}N$ with AlN molar fractions x less than 0.2. Fabrication of optoelectronic devices, which is operated in a much shorter-wavelength region, is also possible using $Al_xGa_{1-x}N$, because wavelengths correspond to their direct band-gap in the range from 360 nm to 200 nm with x changing from 0 to 1. Applications of UV optoelectronics are, e.g., excitation sources for phosphors, light sources of high-density optical memories, fine lithography, and chemical or flame sensing, etc. In order to realize such novel applications, thick $Al_xGa_{1-x}N$ films with high-crystalline quality are necessary. Thick $Al_xGa_{1-x}N$ films are necessary for good optical and carrier confinement in laser diodes or light-emitting diodes and high-sensitivity depletion regions in photodetectors, etc. Usually, sapphire is used as the substrate for the epitaxial growth of $Al_xGa_{1-x}N$. When $Al_xGa_{1-x}N$ is directly grown on a sapphire substrate, however, it is difficult to grow single-crystal films of good crystalline quality due to the large lattice and thermal expansion coefficient mismatches. Several kinds of buffer layers are induced to reduce the strain and avoid cracks.[4,5]

Rutherford backscattering (RBS) is a powerful nuclear technique to characterize the composition, thickness, and interface of films directly and nondestructively;[6–8] it gives more reliable compositions in AlGaN and InGaN layers than methods conventionally used in this field, such as X-ray diffraction (XRD) and photoluminescence.[9,10] When the ion beam is directed along a high-symmetry crystal direction, a phenomenon called "channeling" occurs. The incident ion beam will undergo a series of correlated small-angle scatterings and consequently the backscattering significantly reduces compared with the backscattering when the ion beam is directed in a random direction. $\chi_{\min}$, which is the ratio of the backscattered yield when aligned to a crystallographic axis (Y_A) to that to the random direction (Y_R), is a measure of the crystalline quality of the film. RBS combined with channeling can provide useful information such as the crystalline quality and the defect density profile. Moreover, the angular scan around an off-axis can determine the tetragonal distortion induced by the elastic strain in an epilayer. Due to the depth sensitivity of this technique, RBS/channeling can determine the strain in an epilayer as a function of depth, which is impossible with conventional XRD.

In this paper, we first describe the chemical compositions and the thickness of an $Al_{0.2}Ga_{0.8}N$ epilayer with an AlN interlayer determined by RBS. Then, the high crystalline quality of the AlGaN layer is characterized with the combination of RBS and channeling. In addition, a quantitative analysis of the tetragonal distortion and its depth dependence in the epilayer is shown to give direct experimental evidence for strain relaxation in the $Al_{0.2}Ga_{0.8}N$ epilayer by the AlN interlayer.

*Project supported by the National Natural Science Foundation of China (Grant No. 91226202).
†Corresponding author. E-mail: sdyao@pku.edu.cn
© 2014 Chinese Physical Society and IOP Publishing Ltd

2. Experimental

The AlGaN layer was grown at 1150 °C by metal–organic chemical vapor deposition (MOCVD) using a thick GaN layer as a template. The temperature was decreased to 650 °C during the growth of the AlN interlayer. The precursors for AlN and AlGaN were trimethylaluminum (TMAl), trimethylgallium (TMGa), and ammonia (NH_3), respectively. N_2 was used as the carrier gas during the growth. A collimated 2.023 MeV He^+ beam produced by a 5SDH-2 Pelletron was used for the RBS/channeling measurements. The backscattered particles were detected at 165° with respect to the beam direction by using a Au–Si barrier detector with the energy resolution about 18 keV, corresponding to a depth resolution of about 1 nm. High resolution X-ray diffraction (HRXRD) measurement was carried out on the Beijing synchrotron radiation facility 1W1A system. The X-ray wavelength was 1.541 Å.

3. Results and discussion

Figure 1 shows the random and aligned RBS spectra of this sample. The inset shows the geometry used in the backscattering measurements. The vertical arrow labeled Ga indicates the energy of the He^+ ion backscattered from Ga atoms on the surface. A simulation of the random spectrum given by the RUMP program[11] reveals that a 400-nm $Al_{0.2}Ga_{0.8}N$ layer with a 10-nm AlN interlayer was on the thick GaN layer. The pit on the random backscattered spectrum around a backscattering energy at 1.32 MeV indicates that the depth of the AlN interlayer is 200 nm. The [0001] aligned spectrum of Ga atoms shows that $\chi_{\min}$ of the $Al_{0.2}Ga_{0.8}N$ layer is 1.4%, which means this layer has a high crystalline quality.

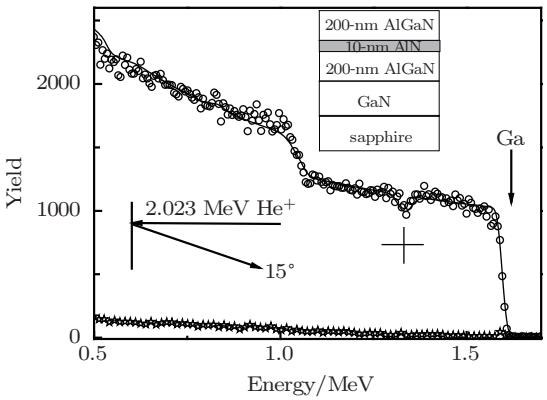


Fig. 1. Random (○), aligned (⋆), and simulated (solid line) RBS spectra along [0001] of the $Al_{0.2}Ga_{0.8}N/AlN/Al_{0.2}Ga_{0.8}N$ heterostructure.

Figure 2(a) shows a symmetric HRXRD measurement obtained from this sample, with 2θ ranging from 125° to 130° (including the GaN (0006) and AlGaN (0006)). The separated diffraction peak of AlGaN is probably caused by the different elastic strain in the AlGaN layers. By using Vegard's law[12] and the lattice constants of bulk AlN (a_b = 0.3111 nm, c_b = 0.4978 nm) and bulk GaN (a_b = 0.3189 nm, c_b = 0.5185 nm), a_b = 0.3173nm, c_b = 0.5144 nm for bulk (fully relaxed) $Al_{0.2}Ga_{0.8}N$ are obtained. Taking the position of the Al_2O_3 (0006) peak (not shown) as a reference, the position of the fully relaxed $Al_{0.2}Ga_{0.8}N$ (0006) peak is shown in Fig. 2. The lattice constants c_{epi} of the AlGaN layers are calculated to be 0.5136 ± 0.0001 nm and 0.5128 ± 0.0001 nm, respectively, which are smaller than the bulk one c_b. It indicates that the perpendicular stain of the epilayers $e^{\perp} = (c_{epi} - c_b)/c_b$ is negative, i.e., the AlGaN layers are under compressive strain, which equal to $-0.15\% \pm 0.02\%$ and $-0.31\% \pm 0.02\%$, in the perpendicular direction.

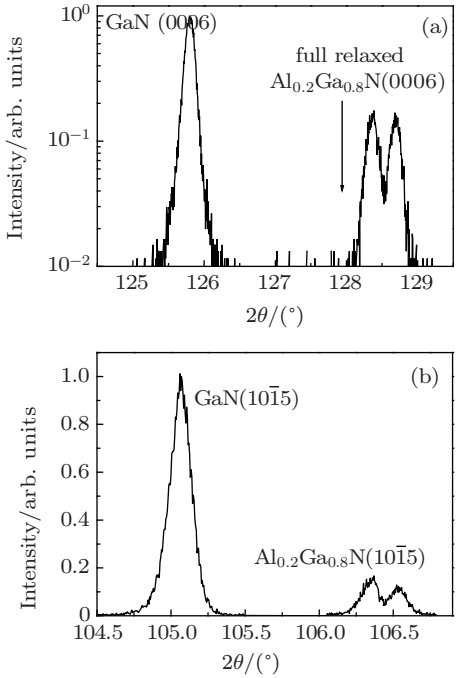


Fig. 2. High resolution X-ray diffraction $2\theta/\omega$ scan curves of (0006) (a) and (10$\bar{1}$5) (b).

The in-plane lattice constant, a_{epi}, is determined from $2\theta/\omega$ scans of the (10$\bar{1}$5) diffraction (Fig. 2(b)) combined with the results from (0006) scans. According to the d spacing equation for a hexagonal crystal

$$d_{hkl} = \frac{1}{\sqrt{\frac{4}{3}\left(\frac{h^2+hk+k^2}{a^2}\right)+\left(\frac{l^2}{c^2}\right)}} \quad (1)$$

substituting the measured values of $d(10\bar{1}5)$, $c = c_{epi}$, and $h = 1$, $k = 0$, $l = 5$ into Eq. (1), we obtain the values of a_{epi} and the estimated errors. From these values, the parallel strain of the AlGaN layers $e^{\parallel} = (a_{epi} - a_b)/a_b$ is deduced to be 0.10% ± 0.04% and 0.22% ± 0.04%, respectively. Thus, the tetragonal distortion $e_T = e^{\parallel} - e^{\perp}$ of the AlGaN layers is deduced to be 0.25% ± 0.06% and 0.53 ± 0.06%.

To study the depth-dependent tetragonal distortion of the AlGaN layer, the off-normal axis [1$\bar{2}$13] is chosen. Figure 3 shows the aligned spectrum along the [1$\bar{2}$13] axis, the random spectrum, and the simulated spectrum. The $\chi_{\min}$ in Fig. 3 is 2.9%, which is larger than the value in Fig. 1, because the index of this axis is higher. After the orientations of the (10$\bar{1}$0) plane and the [1$\bar{2}$13] axis are found, the sample is tilted step by step in the (10$\bar{1}$0) plane around the [1$\bar{2}$13] axis direction from $-2.0°$ to $2.0°$ with a step size of $0.1°$. Thus 41 RBS spectra were obtained, with each one corresponding to a specific tilt angle to the [1$\bar{2}$13] axis. Six energy windows were chosen (W1–W6) in the RBS spectra, corresponding to six different depth regions in the AlGaN layer, as shown in Fig. 3. Using the data from the 41 RBS spectra, six angular scans around the [1$\bar{2}$13] axis were obtained, each one related to a specific depth region defined by the energy window. As an example, the angular scan corresponding to the energy window W1 is shown on the right-hand side in Fig. 4. Fitting with a Gaussian function is used to accurately determine the position of the dip (dashed line). On the left-hand side of Fig. 4, an angular scan in the (10$\bar{1}$0) plane around the [0001] axis is shown. The center of the [0001] dip is not depth-dependent, because the tetragonal distortion only influences the orientation of off-normal axes but not the [0001] axis. The inset in Fig. 4 schematically shows that the direction of the [1$\bar{2}$13] axis on the (10$\bar{1}$0) plane (which also contains [0001] and [11$\bar{2}$0] axes) will be changed when there is tetragonal distortion. From Fig. 4, we can calculate the angle between the [0001] and the [1$\bar{2}$13] axes at a depth of 360 nm of the AlGaN epilayer $\Phi_{\rm epi} = \tan^{-1}(a_{\rm epi}/c_{\rm epi}) = 32.27° - 0.43° = 31.84° \pm 0.01°$, where $a_{\rm epi}$ and $c_{\rm epi}$ are the lattice constants of the AlGaN epilayer. The value of Φ is equal to $\tan^{-1}(a/c)$ (as shown in the inset of Fig. 4), which is $\Phi_{\rm b} = \tan^{-1}(a_{\rm b}/c_{\rm b}) = 31.67°$ for bulk (fully relaxed) $Al_{0.2}Ga_{0.8}N$. Therefore, $\Delta\Phi = \Phi_{\rm epi} - \Phi_{\rm b} = 0.17° \pm 0.02°$ and the tetragonal distortion $e_{\rm T} = e^{\parallel} - e^{\perp} = \Delta\Phi / \sin\Phi_{\rm b}\cos\Phi_{\rm b} = 0.66\% \pm 0.08\%$ can be determined, where $e^{\parallel}$ and $e^{\perp}$ are the parallel and perpendicular elastic strain of the epilayer.

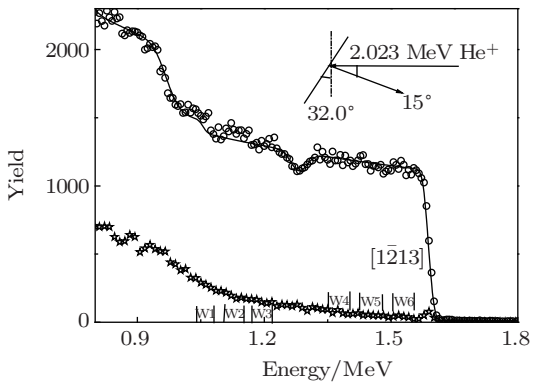


Fig. 3. Random (○), [1$\bar{2}$13] aligned (⋆), and simulated (solid line) RBS spectra of the sample. The backscattering geometry and six energy windows (W1 to W6) used for the plots of angular scans are also presented.

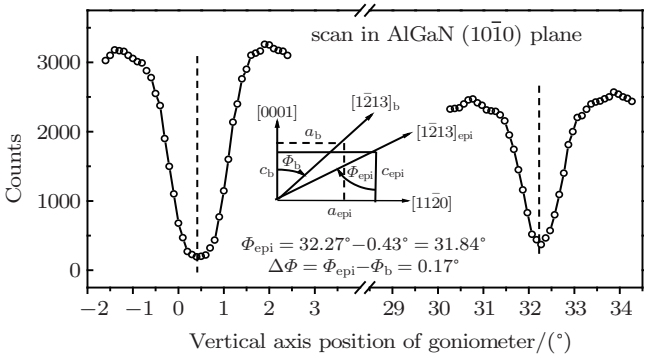


Fig. 4. Angular scans along the $Al_{0.2}Ga_{0.8}N$ (10$\bar{1}$0) plane corresponding to a depth of 340 nm (W1).

Table 1. Strain related data, $\Delta\Phi$ and $e_{\rm T}$ at different depths.

Window	W1	W2	W3	W4	W5	W6
Depth/nm	360	300	240	150	90	30
$\Delta\Phi$/(°)	0.17	0.16	0.15	0.08	0.07	0.07
$e_{\rm T}$/%	0.66	0.62	0.59	0.27	0.21	0.21

Table 1 shows $\Delta\Phi$ and $e_{\rm T}$ obtained with different depths in the $Al_{0.2}Ga_{0.8}N$ layer. Figure 5 is a plot of $e_{\rm T}$ with error bar versus the depth. It provides the following information.

(i) The $e_{\rm T}$ (or $\Delta\Phi$) values may be positive or negative, depending on whether the lattice mismatch $\eta = (a_{\rm e} - a_{\rm M})/a_{\rm M}$ is negative or positive, where $a_{\rm e}$ and $a_{\rm M}$ are the lattice constants of epilayer and matrix, respectively. In our case, the lattice mismatch is negative, so the $e_{\rm T}$ (or $\Delta\Phi$) values are positive. It means that the epilayer is under tensile strain in the parallel direction ($e^{\parallel} > 0$) which results in a compressive strain in the perpendicular direction ($e^{\perp} < 0$) due to the elastic properties of the epilayer. In addition, the $e_{\rm T}$ values obtained from XRD are in good agreement with the ones obtained from RBS/channeling.

(ii) The $e_{\rm T}$ values depend on depths. In previous investigations, it was found that for epilayers, the elastic strain is higher in the region close to the interface and decreases gradually towards the surface due to the strain relaxation. However, the tetragonal distortion in AlGaN epilayers decreases sharply after the AlN interlayer. In addition, Pan *et al.*[13] reports that for a strained GaSb/AlSb layer superlattice with many interfaces, the angular scan information obtained in the deeper layer is filtered by the top layer. The real lattice strain should be larger than that measured by angular shift. In our case, such an effect may more or less result in a lower value of $e_{\rm T}$ than the real one in the deeper AlGaN epilayer indicating a more drastic change of the elastic strain in the AlGaN epilayers than the measured one. Therefore, the AlN interlayer plays an important role in the strain reduction of the AlGaN epilayer. Given the fact that the dechanneling rate increases obviously below the AlN interlayer (see Fig. 3), a high density of lattice dislocation is speculated to be formed at the AlN/AlGaN interface, leading to a strain relaxation in the upper AlGaN layer.[14] In addition, the lattice mismatch ($\eta = -2.0\%$) between the AlN

interlayer and a deeper $Al_{0.2}Ga_{0.8}N$ layer is larger than the one ($\eta = -0.5\%$) between $Al_{0.2}Ga_{0.8}N$ and GaN, thus the strain relaxation in AlN is also expected to be faster. This can also be a reason leading to a relatively smaller tetragonal distortion in the upper AlGaN layer.

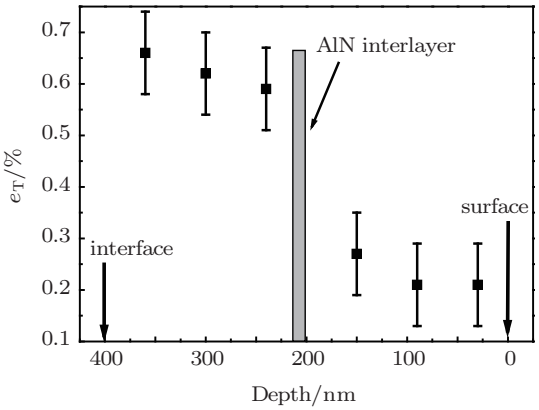


Fig. 5. The depth-dependence of e_T of the AlGaN epilayer measured by RBS/channeling.

4. Conclusions

A good quality ($\chi_{min} = 1.4\%$) of 400-nm $Al_{0.2}Ga_{0.8}N$ layer with an AlN interlayer was prepared on sapphire with a thick GaN intermediate layer by MOCVD. RBS/channeling is useful to characterize the structure of the epilayer, especially since it is indispensable to study the depth-dependence of the strain the epilayer. According to the result we obtained, it is expected that the AlN interlayer can be used to reduce the elastic strain and enhance the crystalline quality of the AlGaN epilayer. This study again proves RBS/Channeling as a powerful method in the characterization of multi-layered thin films.

References

[1] Amano H, Sawaki N, Akasaki I and Toyoda Y 1986 *Appl. Phys. Lett.* **48** 353
[2] Amano H, Kitoh M, Hiramatsu K and Akasaki I 1990 *J. Electrochem. Soc.* **137** 1639
[3] Amano H, Kito M, Hiramatsu K and Akasaki I 1989 *Jpn. J. Appl. Phys.* **28** L2112
[4] Koide Y, Itoh N, Itoh K, Sawaki N and Akasaki I 1988 *Jpn. J. Appl. Phys.* **27** 1156
[5] Simth M D, Sadler T C, Li H N, Zubialevich V C and Parbrook P J 2013 *Appl. Phys. Lett.* **103** 081602
[6] Chu W K, Mayer J W and Nicolet M A 1978 *Backscattering Spectrometry* (New York: Academic)
[7] Wang H, Yao S D, Pan Y B and Zhang G Y 2007 *Acta Phys. Sin.* **56** 3350 (in Chinese)
[8] Wang H, Chen T X and Yao S D 2008 *Nucl. Instrum. Methods B* **266** 1141
[9] Wu M F, Vantomme A, Hogg S, Pattyn H, Langouche G, van der Stricht W, Jocobs K and Moerman I 1999 *Appl. Phys. Lett.* **74** 365
[10] Wu M F, Yao S D, Vantomme A, Hogg S, Langouche G, Li J and Zhang G Y 1999 *J. Vac. Sci. Technol. B* **17** 1502
[11] Doolittle L R 1985 *Nucl. Instrum. Methods Phys. Res. B* **9** 344
[12] Williams C K, Glisson T H, Hauser J R and Littlejohn M A 1978 *J. Electron. Mater.* **7** 639
[13] Pan C K, Zheng D C, Finstad T G, Chu W K, Speriosu V S, Nicolet M A and Barrett J H 1985 *Phys. Rev. B* **31** 1270
[14] Reiher A, Blasing J, Dadgar A, Diez A and Krost A 2003 *J. Cryst. Growth* **248** 563